Diurnal cycle of water vapor and clouds profiles observed from space, comparison with one GCM

H. Chepfer , H. Brogniez, V. Noel, R. Guzman

Sorbonne Université, Université Versailles-Saint-Quentin,
CNRS, Ecole Polytechnique

The cloud and water vapor diurnal cycles

Wood, R. Stratocumulus clouds. (2012).
Nuijens, L., Stevens, B. & Siebesma, A.P. The Environment of Precipitating Shallow Cumulus Convection. (2009).
Kollias, P. & Albrecht, B. Vertical Velocity Statistics in Fair-Weather Cumuli at the ARM TWP Nauru Climate Research Facility. (2010).
Ruppert, Jr. J. H. & Johnson, R. H. On the cumulus diurnal cycle over the tropical warm pool. (2016).
Gray, W.M. & Jacobson, R.W. Diurnal Variation of Deep Cumulus Convection. (1977).
Noel, V., et al. The diurnal cycle of cloud profiles over land and ocean between 51° S and 51° N, (2018).
Wallace, J. M. Diurnal Variations in Precipitation and Thunderstorm Frequency over the Conterminous United States. (1975).
Randall, D. A., Harshvardhan & Dazlich, D. A. Diurnal Variability of the Hydrologic Cycle in a General Circulation Model. (1991).
Chen, S. S. & Houze, R. A. Diurnal variation and life-cycle of deep convective systems over the tropical pacific warm pool. (1997).
Tian, B. et al. Diurnal cycle of convection, clouds, and water vapor in the tropical upper troposphere: Satellites versus a general circulation model. (2004).
Stubenrauch, et al. . Cloud Properties and Their Seasonal and Diurnal Variability from TOVS Path-B. (2006).
Wang, et al J. A near-global, 2-hourly data set of atmospheric precipitable water from ground-based GPS measurements. (2007).
Wylie, D. Diurnal Cycles of Clouds and How They Affect Polar-Orbiting Satellite Data. (2008).
Minnis, P. & Harrison, E. F. Diurnal variability of regional cloud and clear-sky radiative parameters derived from GOES data (1984).
Rozendaal, et al. A. An Observational Study of Diurnal Variations of Marine Stratiform Cloud. (1995).
Soden, B. J. The diurnal cycle of convection, clouds, and water vapor in the tropical upper troposphere. (2000).
Wood, et al. D. L. Diurnal cycle of liquid water path over the subtropical and tropical oceans. (2002).
Taylor, S., et al. M. Evaluating the diurnal cycle in cloud top temperature from SEVIRI, (2017).
Shang, H. & al. Diurnal cycle and seasonal variation of cloud cover over the Tibetan Plateau, (2018).
Clark, A. J., et al. T. C. Comparison of the diurnal precipitation cycle in convection-resolving and non-convection-resolving mesoscale models. (2007).
Pfeifroth, et al. B. Cloud cover diurnal cycles in satellite data and regional climate model simulations. (2012).
Webb, M. J. et al. The diurnal cycle of marine cloud feedback in climate models. (2015).
Yin J. & Poporato. A. Diurnal cycle cloud cycle biases in climate models (2018).
Yang, G.-Y. & Slingo, J. The diurnal cycle in the tropics. *Mon. Weather Rev.* **129**, (2001).
Moradi, et al. E. Diurnal variation of tropospheric relative humidity in tropical regions. (2016).
Eriksson, P. et al. Diurnal variations of humidity and ice water content in the tropical upper troposphere. (2010).
Kottayil, A., et al. Correcting diurnal cycle aliasing in satellite microwave humidity sounder measurements. (2013).
Kottayil, A., et al. K. Evaluating the diurnal cycle of upper tropospheric humidity in two different climate models using satellite observations, (2016).
Sui, C., et al. Diurnal Variations in Tropical Oceanic Cumulus Convection during TOGA COARE. (1997).
Bastin, S., et al. . Diurnal Cycle of Water Vapor as Documented by a Dense GPS Network in a Coastal Area during ESCOMPTE IOP2. (2007).
Sakaeda, et al. The Diurnal Variability of Precipitating Cloud Populations during DYNAMO. (2018).
Zhao, W., et al. The diurnal cycle of clouds and precipitation at the ARM SGP site: Cloud radar observations and simulations from the multi-scale modeling framework (2017).
Vial et al. A new look at the diurnal cycle of tradewind cumulii.(2019)
….

The global view of the cloud diurnal cycle has changed recently

Before

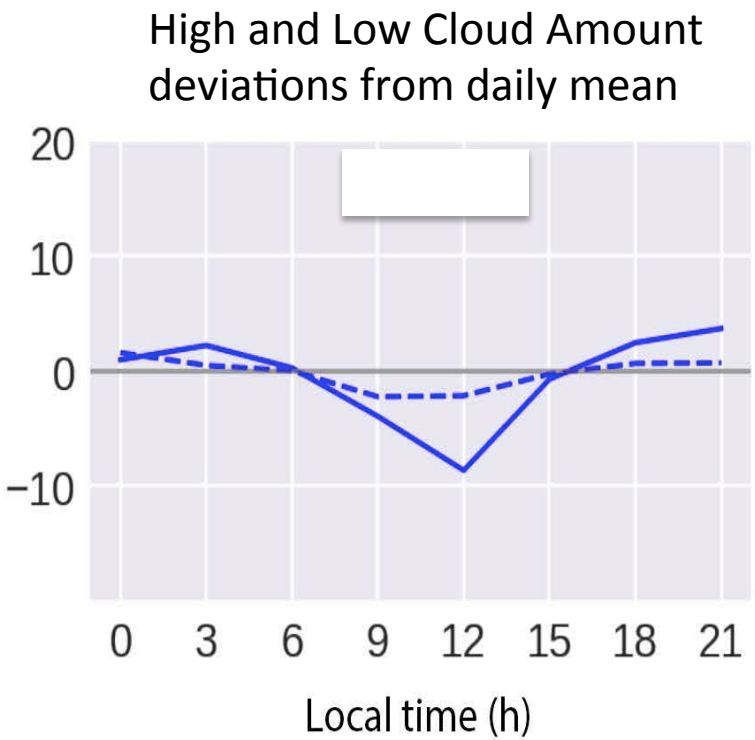

Now

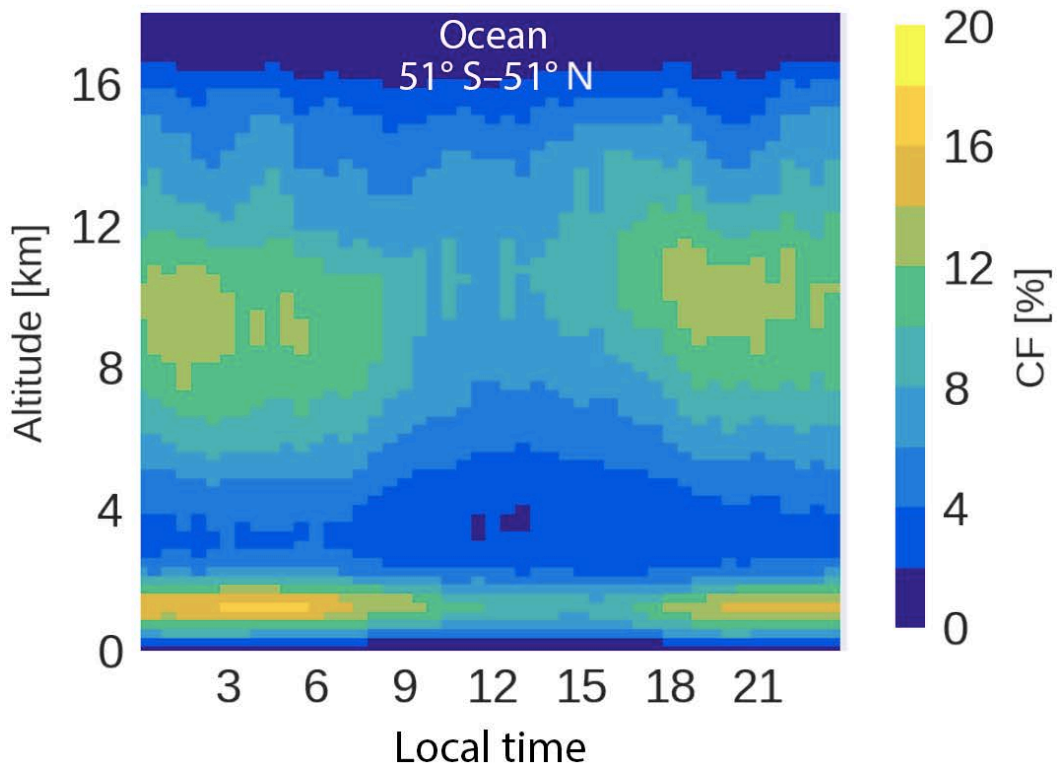

Noel, V., H. Chepfer, M. Chiriaco, C. York, 2018: The diurnal cycle of cloud profiles over land and ocean between 51° S and 51° N…, *Atmos. Chem. Phys*. **18**, 9457-9473 (2018).

1) Observe how the Relative Humidity profiles and Cloud profiles respond to the solar diurnal forcing across the Tropics

2) Test the model physic

1) Observe how the Relative Humidity profiles and Cloud profiles respond to the solar diurnal forcing across the Tropics

2) Test the model physic

Observations collected recently by low-orbiting satellites => diurnal cycle

- Relative Humidity Profiles from SAPHIR on-board the Megha-Tropiques (Brogniez et al. 2011)
- OLR from ScaRaB instrument on-board the Megha-Tropiques satellite (Roca et al. 2015)
- Cloud profiles from CATS Lidar on-board the International Space Station (York et al. 2019)

Simulations with the LMDz6 GCM with COSPv2/lidar, AMIP type run, high frequency outputs

Time Period: June- July-August 2015-2016-2017

Observations of the diurnal cycles

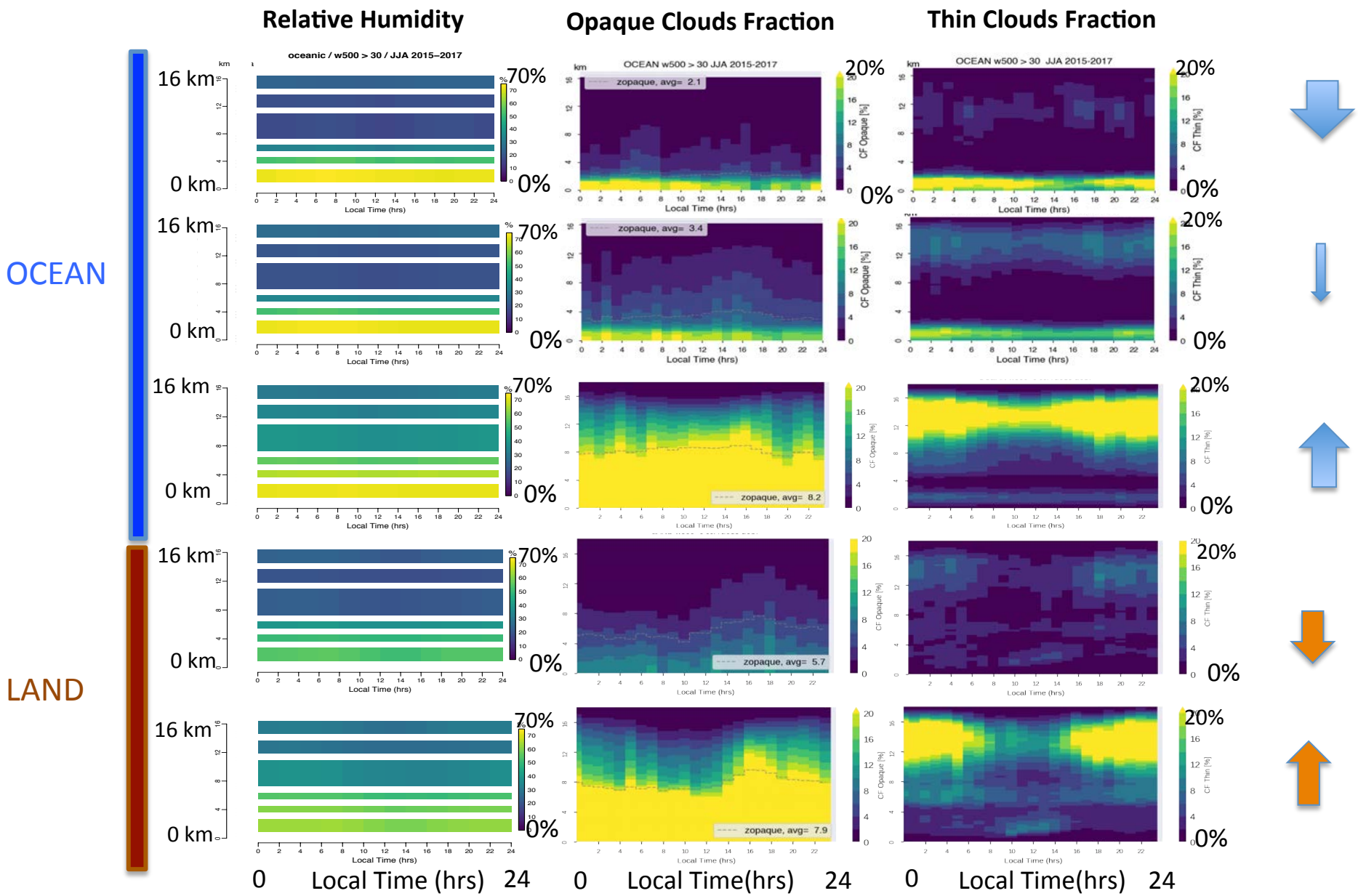

Chepfer et al., under review

Oceanic Ascent: Obs in relative anomaly .wrt. daily mean

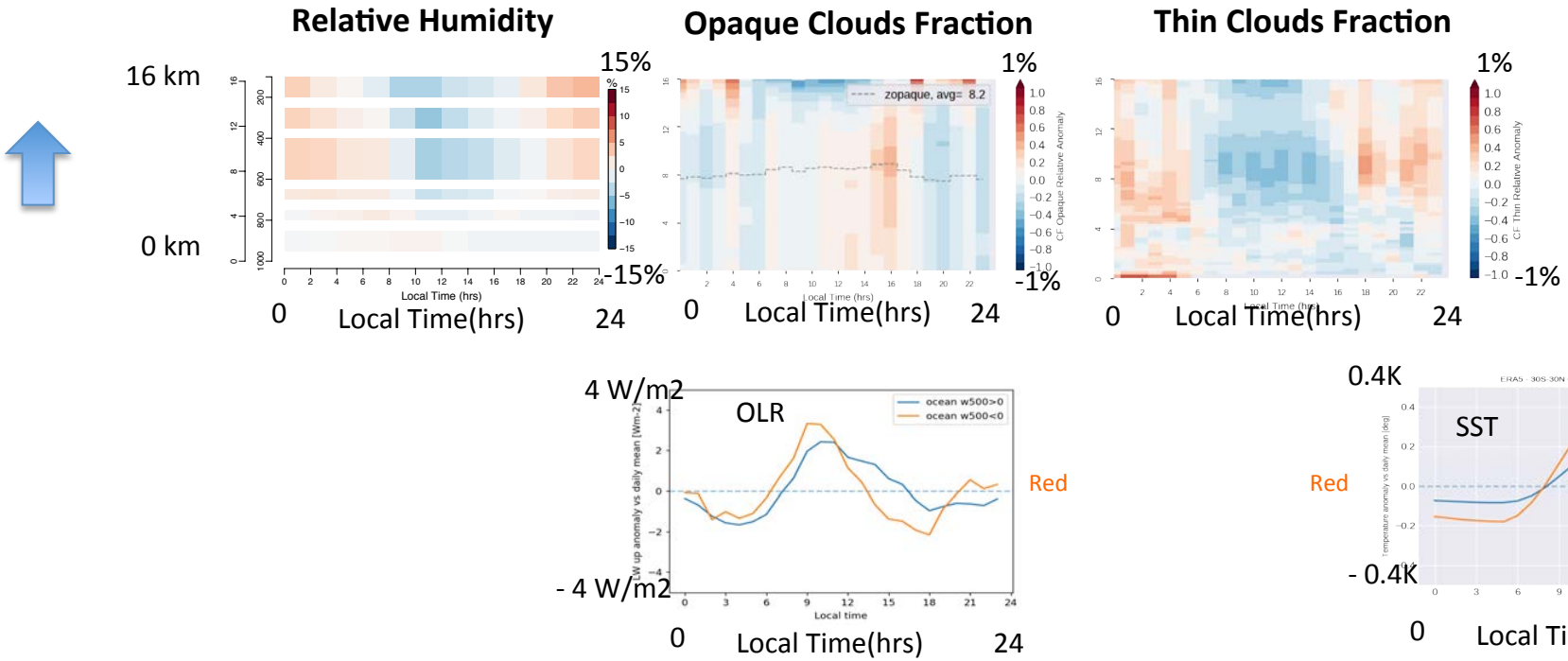

- RH relative anomaly is max in the mid-troposphere at night (15%)
- Cloud relative anomaly is small : max 1%
- Opaque cloud relative anomaly in the mid troposphere in early afternoon (drives the OLR)
- Thin cloud positive relative anomaly in the boundary layer 0-6am and tied to RH in free tropos

Oceanic Ascent: focus on the upper troposphere (> 5 km)

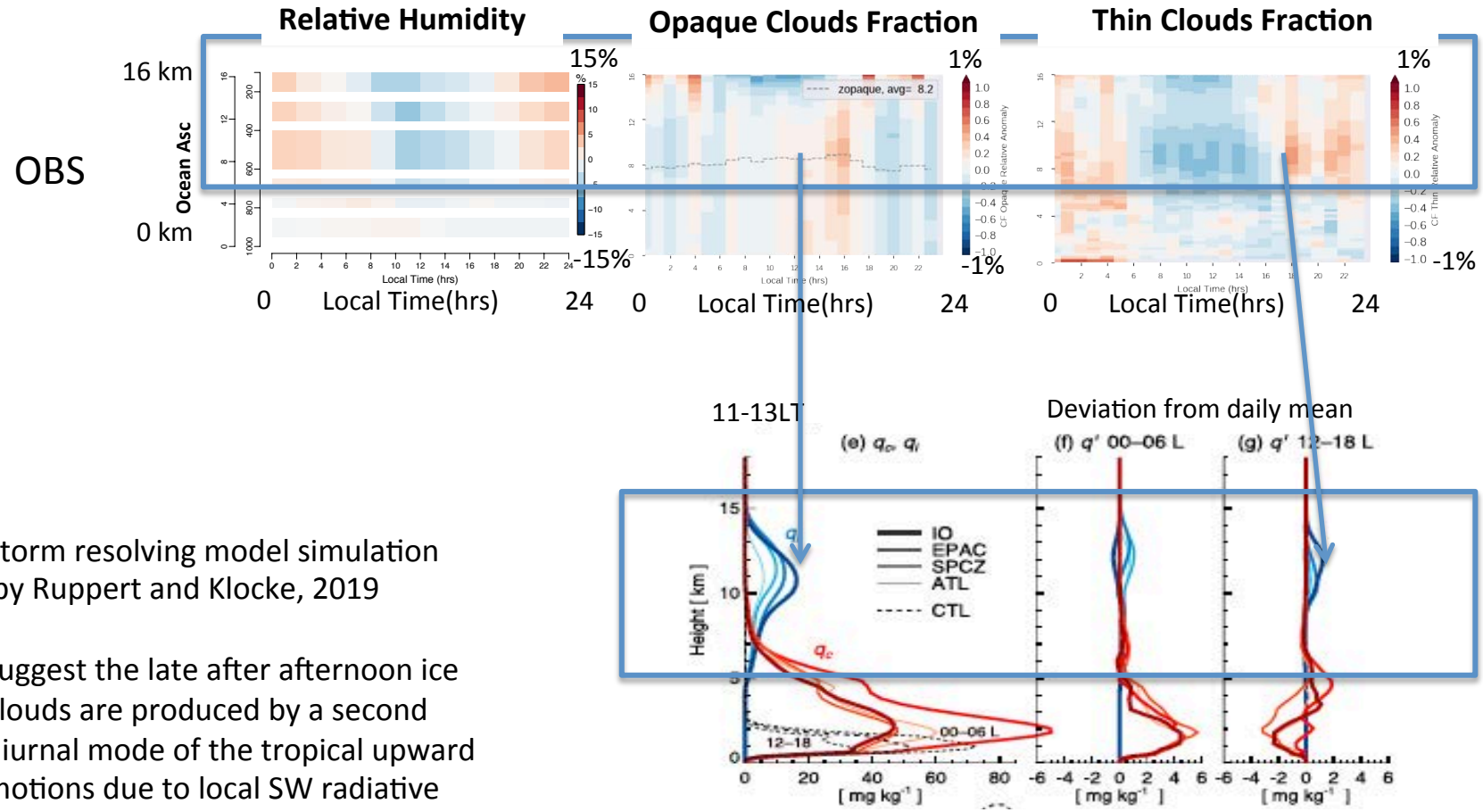

Storm resolving model simulation by Ruppert and Klocke, 2019

suggest the late after afternoon ice clouds are produced by a second diurnal mode of the tropical upward motions due to local SW radiative warming

Oceanic Ascent: focus on the lower troposphere (< 5 km)

OBS

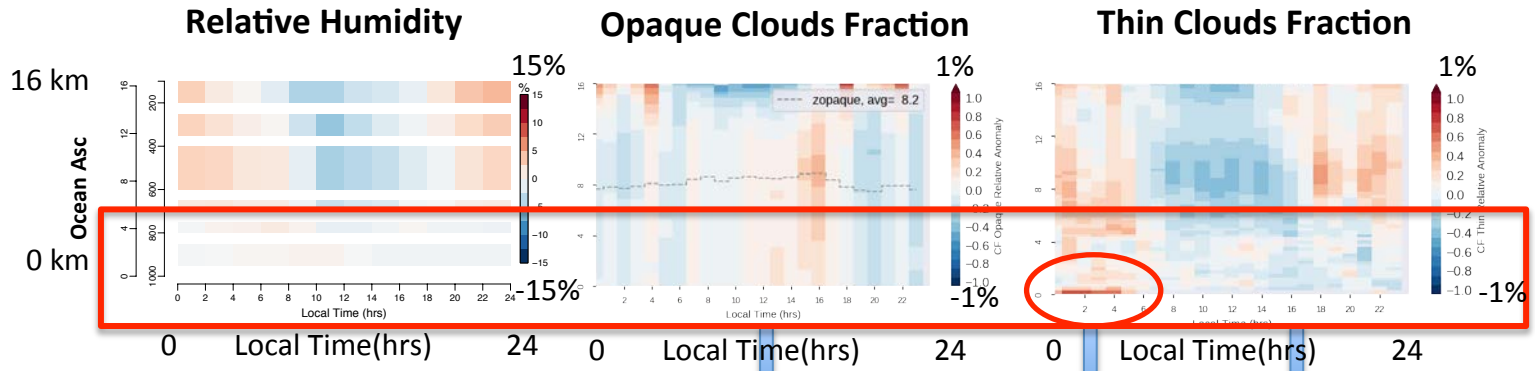

11-13LT

Deviation from daily mean

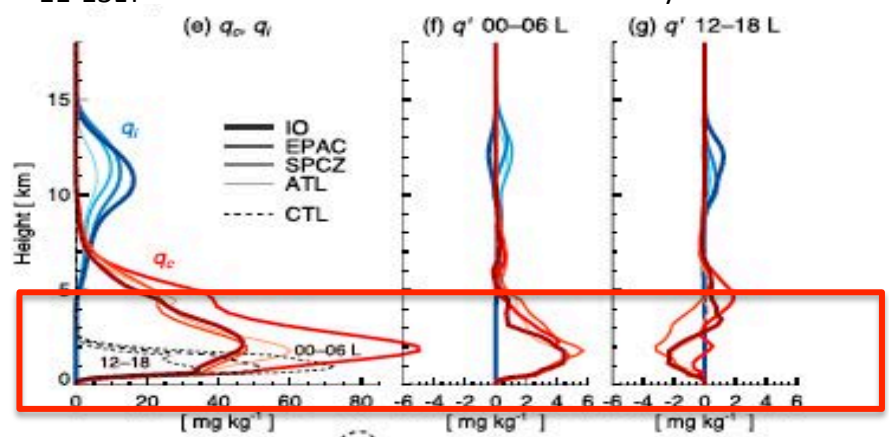

Ruppert and Klocke, 2019

The observations show an enhancement of the condensed water (thin clouds) very close to the surface (<1km) at late night (LW slight surface warming)

Oceanic Ascent: comparison with GCM

OBS

LMDz +COSPv2

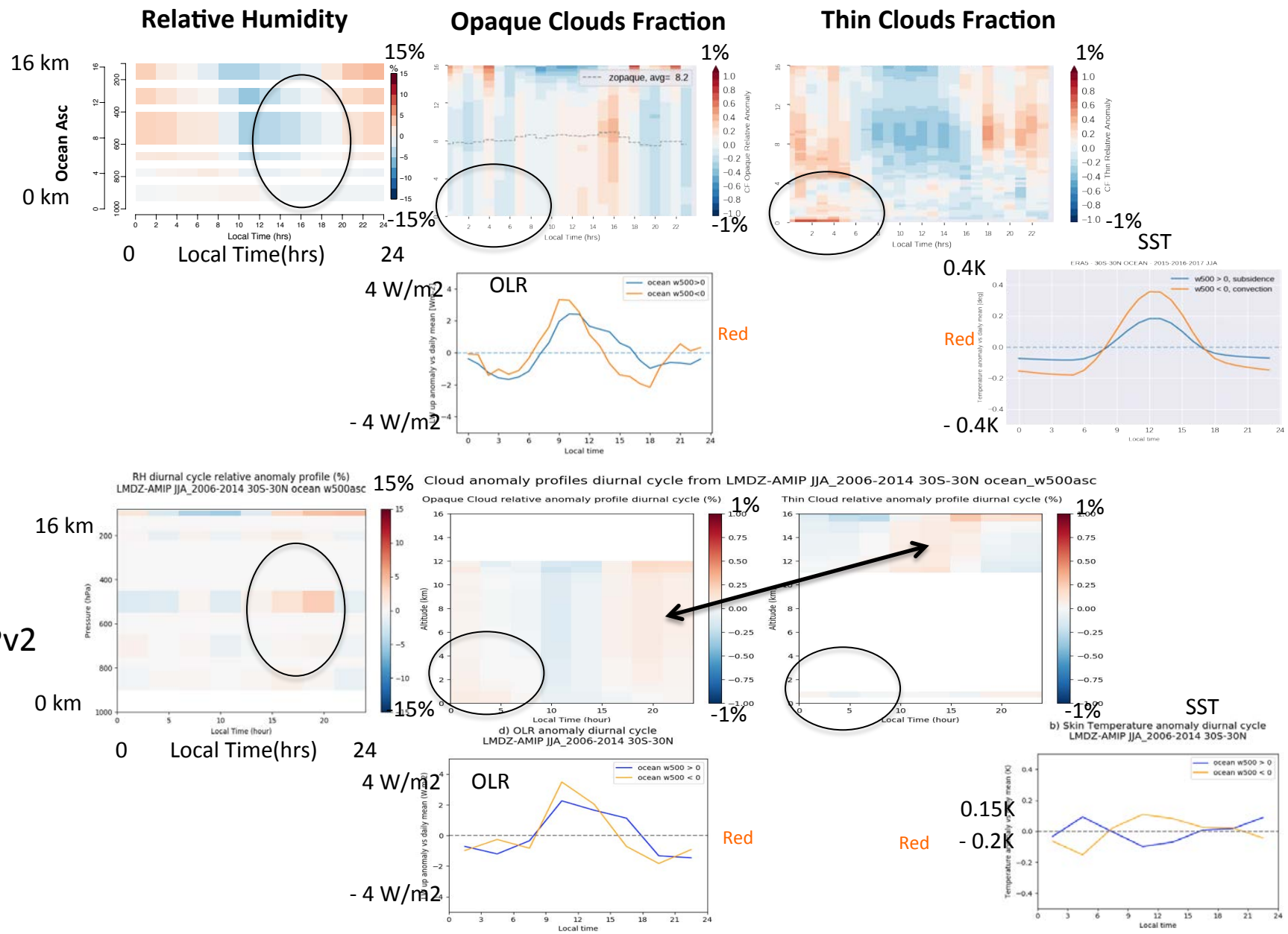

Land Ascent: Obs in relative anomaly .wrt. daily mean

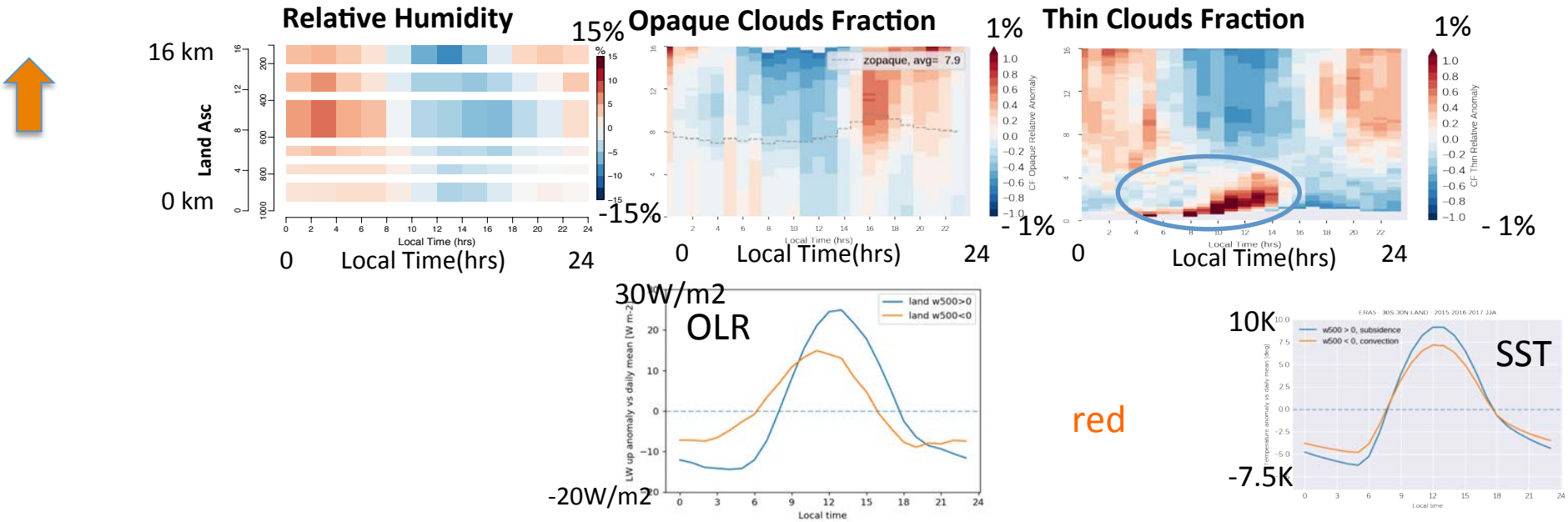

Land Ascending air regions: comparison with GCM

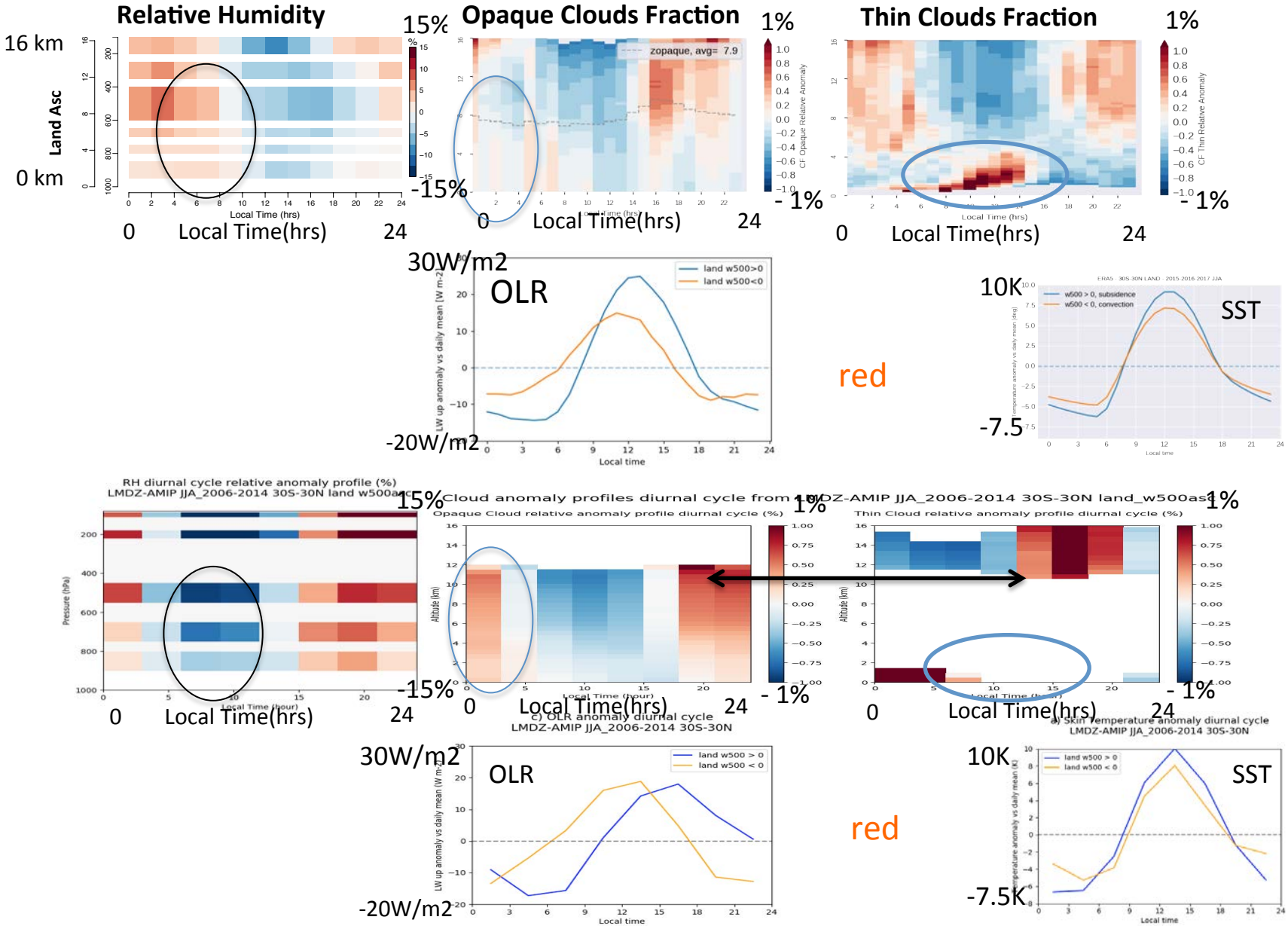

Oceanic moderate subsidence: comparison with GCM

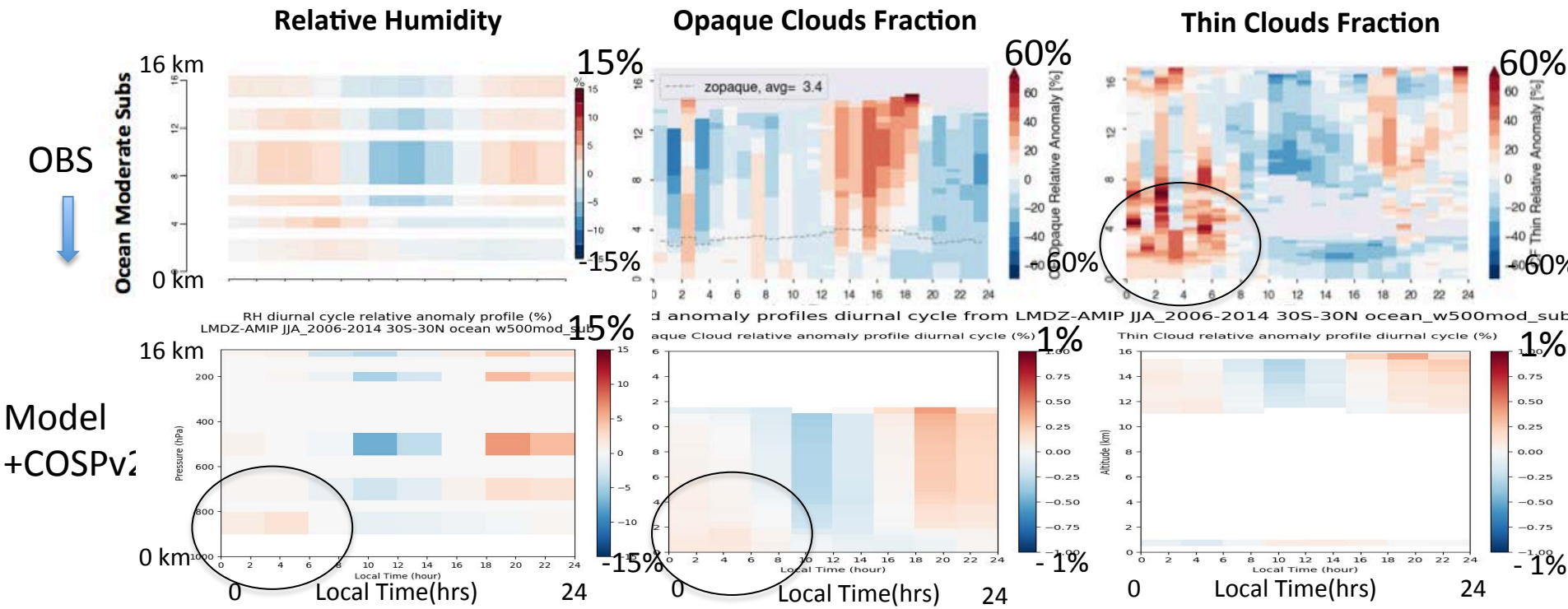

Almost no cloud diurnal cycle in the model (<1%) compared to observations

NB: the model daily mean state is wrong (not shown here)

Summary

- Recent space-borne instruments observe the diurnal cycle of cloud profile and relative humidity profile across the Tropics

- The LMDZ model does not reproduce the observed diurnal cycles.

  The daily mean clouds profile and relative humidity profile are biased in the model (not shown); these biases influence the diurnal cycle biases.

- Does that matter if the diurnal cycle is biased in the model ?

  "some fast processes shape the long term response… based on intuition (cloud changes are fast) and based on examples in the literature"

Supplementary

Daily mean Profiles of HR, Thin Clouds, Opaque Clouds: Obs & Models

Obs

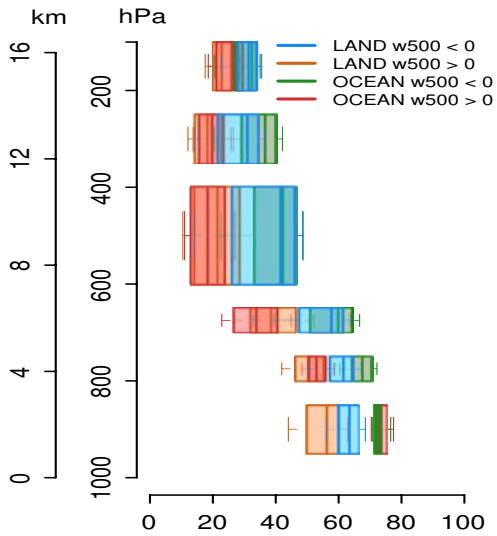

Relative Humidity daily mean profiles
LMDZ-AMIP JJA_2006-2014 30S-30N

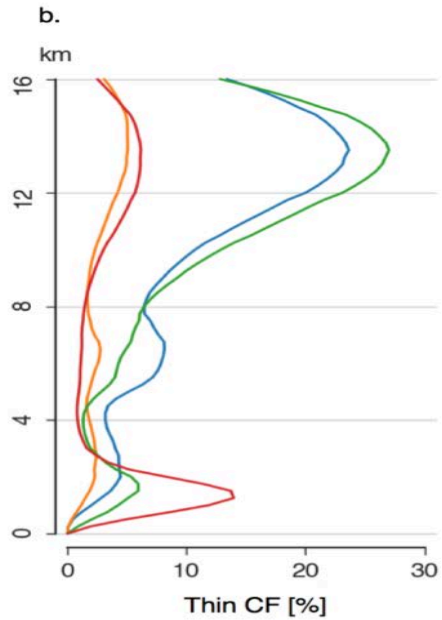

a) Thin cloud fraction daily mean profile
LMDZ-AMIP JJA_2006-2014 30S-30N

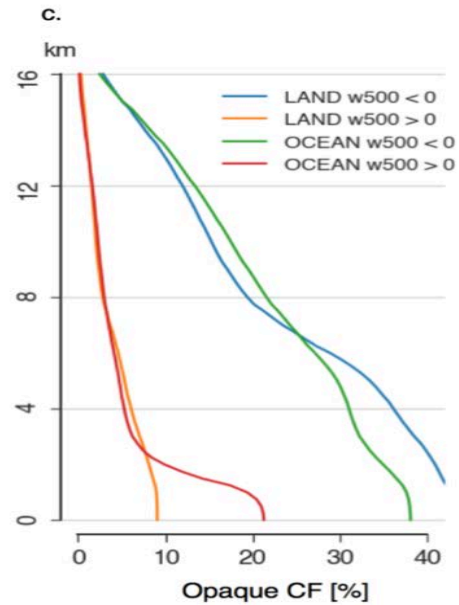

b) Opaque cloud fraction daily mean profile
LMDZ-AMIP JJA_2006-2014 30S-30N

Model+ COSPv2 /lidar

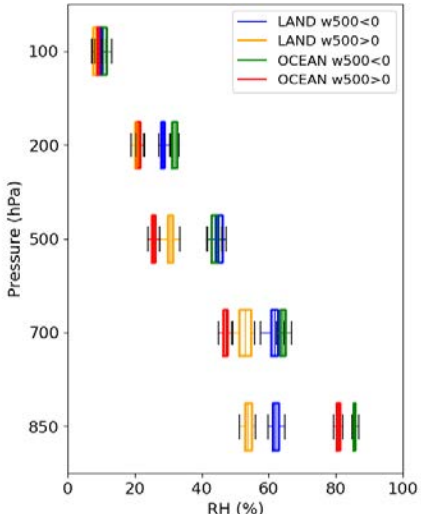

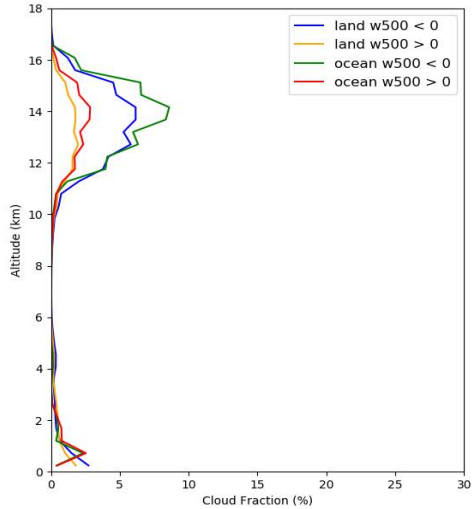

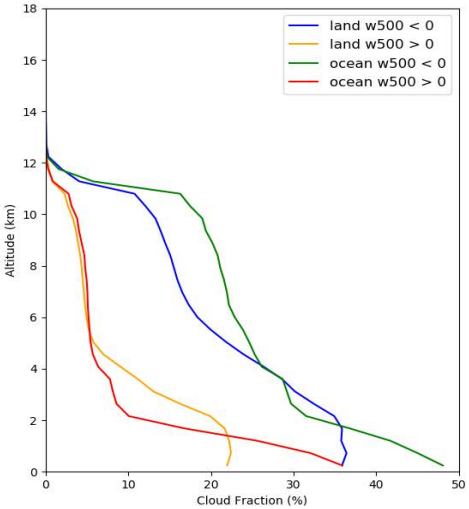

Daily Means Obs & Model

	Land subsidence	Land ascent	Ocean subsidence	Ocean ascent
OLR (W/m2)	275	233	269	238
Absorbed SW (W/m2)	302	276	330	309
Skin Temperature (K)	298.8	298.8	299.9	298.0
Cover Opaque clouds (%)	8.3	30	17.5	27.4
Cover Thin clouds (%)	22.8	40.3	32.2	42.1
Cover Clear sky (%)	68.9	29.7	50.3	30.5
z-opaque (km)	5.7	7.9	3.1	8.2

	Land subsidence	Land ascent	Ocean subsidence	Ocean ascent
OLR (W/m2)	277	252	271	239
Absorbed SW (W/m2)	287	265	301	283
Skin Temperature (K)	299.6	298.5	298.6	299.9
Opaque cloud cover (%)	23.3	37.2	35.9	48.1
Thin cloud cover (%)	6.1	11.4	7.7	12.5
Clear sky cover (%)	70.6	51.4	56.4	39.4
Z_opaque (km)	4.3	6.6	2.7	6.0

Table 1: Daily mean values over the four tropical areas (30°S-30°N) for 9 years of the LMDZ-AMIP+COSPv2 run.

Oceanic subsidence air regions: comparison with GCM

OBS

Ocean Moderate Subs

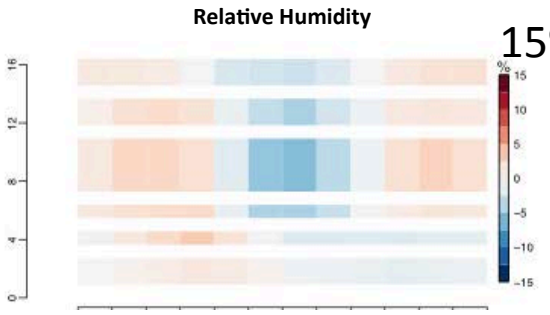

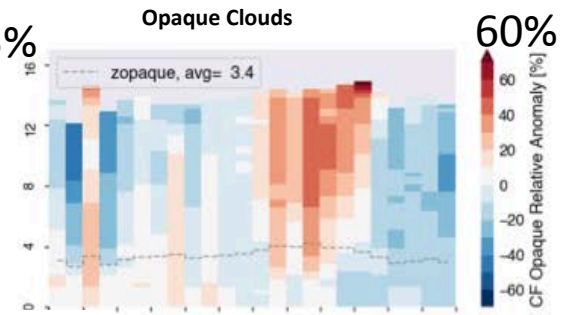

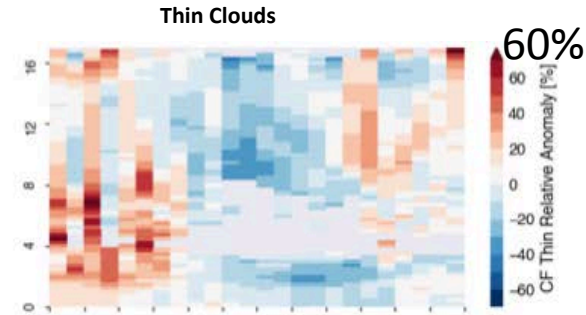

Model +COSPv2

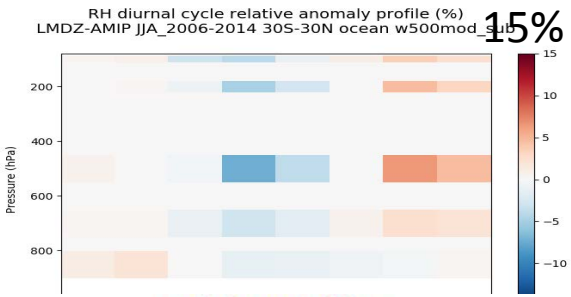

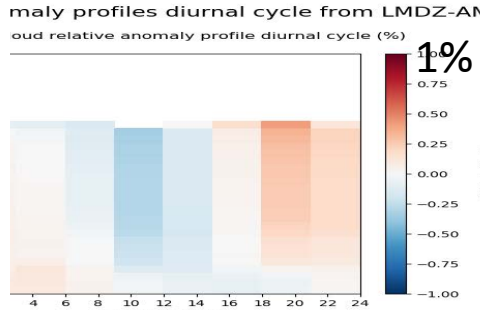

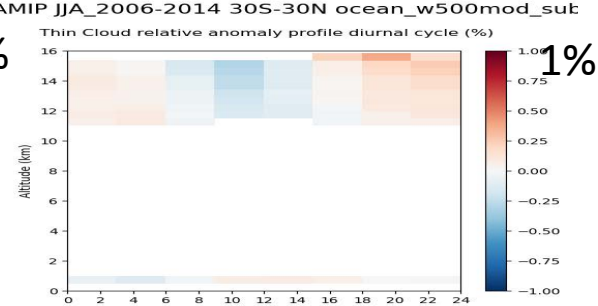

OBS

Ocean Strong Subs

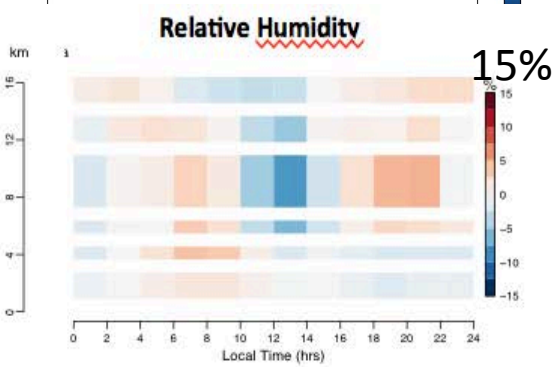

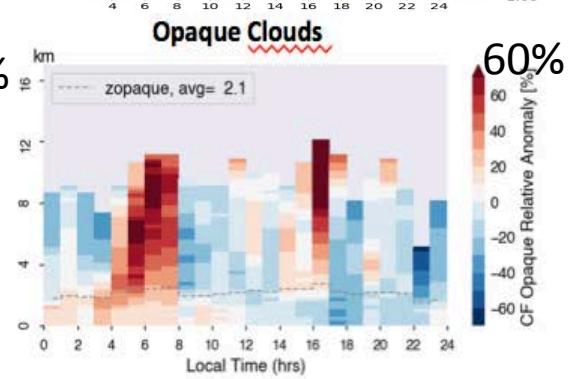

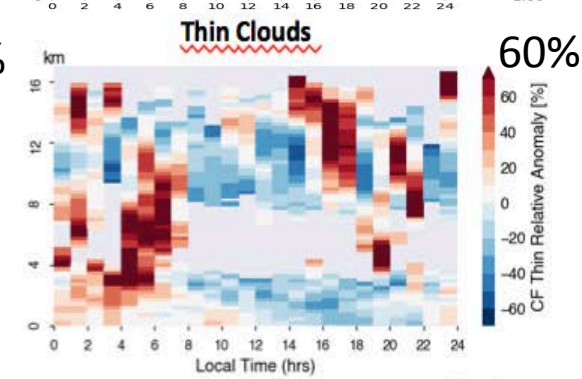

Model +COSPV2/

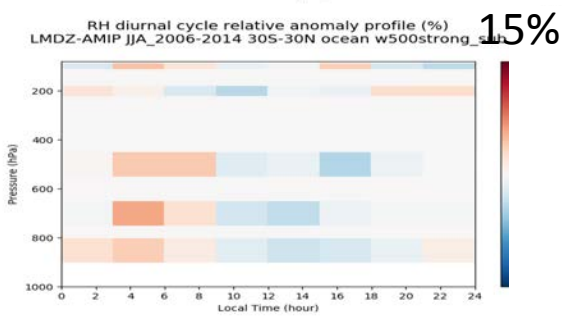

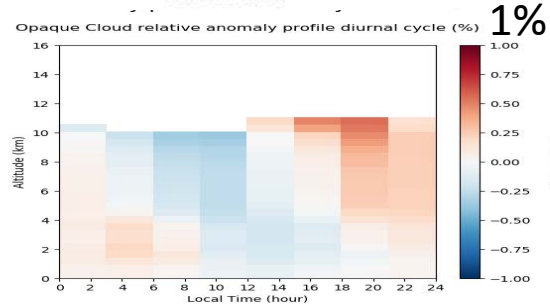

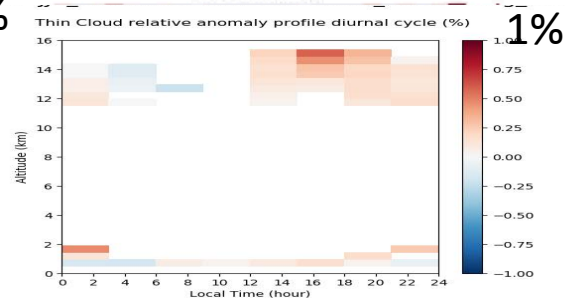

Oceanic Strong subsidence air regions

OBS

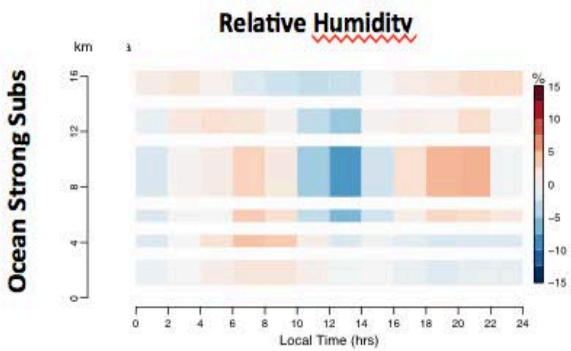

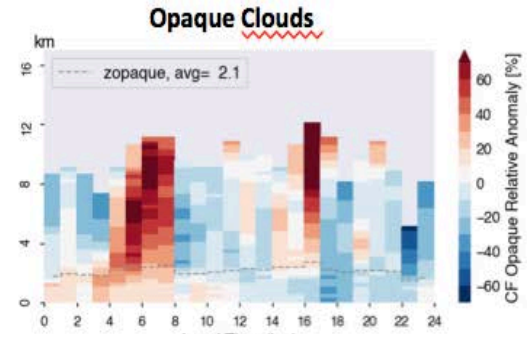

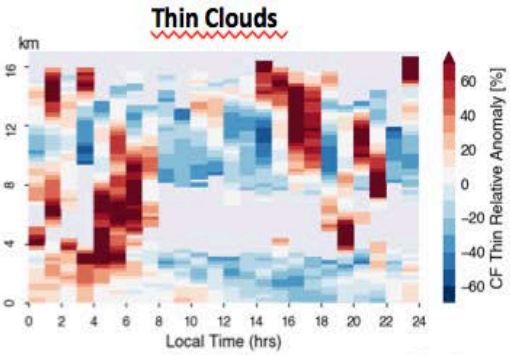

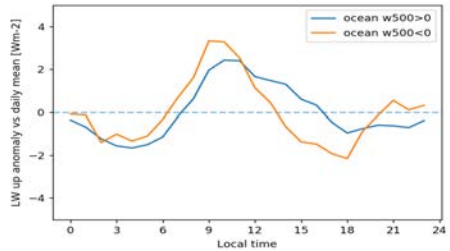

blue

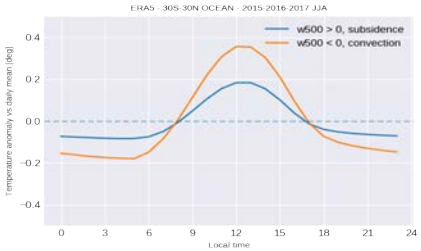

Model +COSP/ lidar

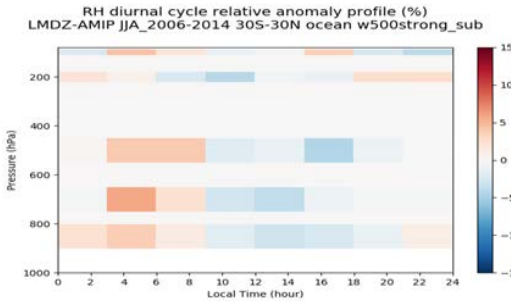

Cloud anomaly profiles diurnal cycle from LMDZ-AMIP JJA_2006-2014 30S-30N ocean_w500strong_sub

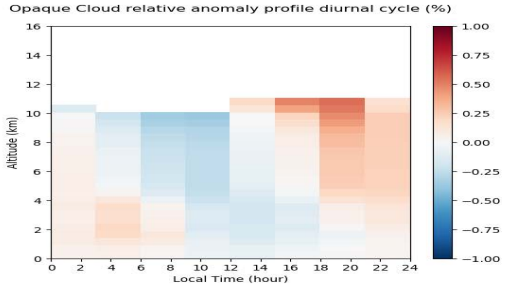

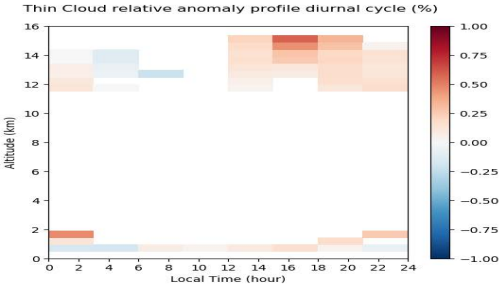

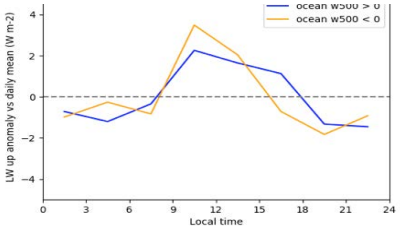

blue

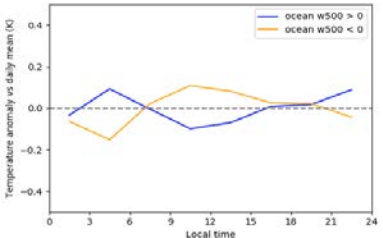

Land Subsiding air regions: in Relative Daily anomalies (equation)

OBS

Model +COSP/ lidar

Relative Humidity

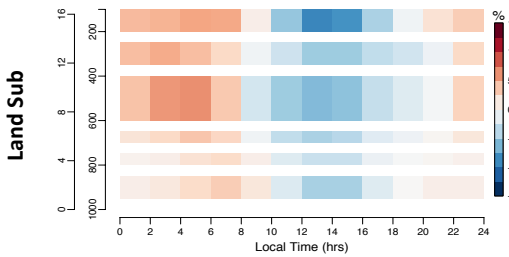

Opaque Clouds

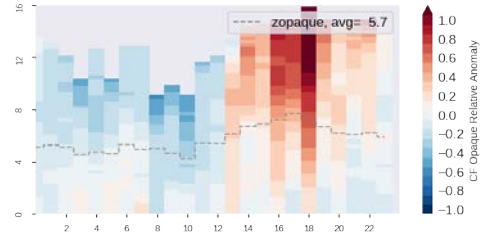

Thin Clouds

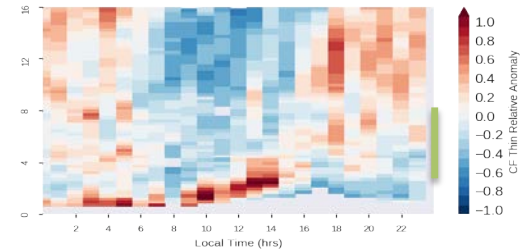

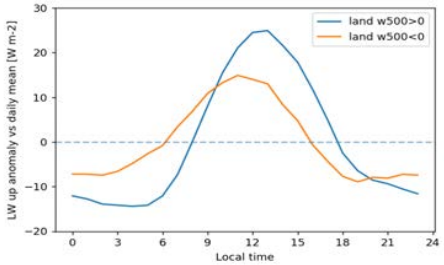

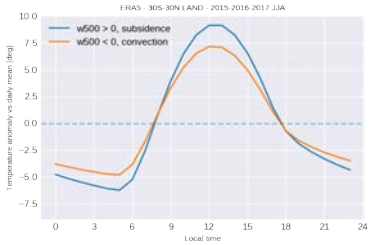

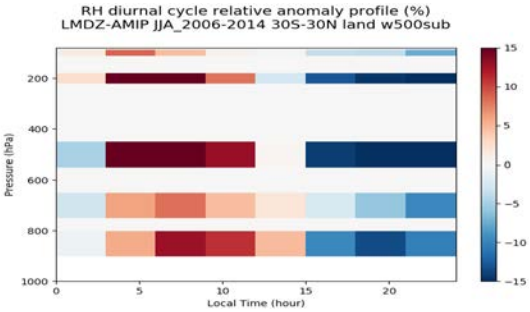

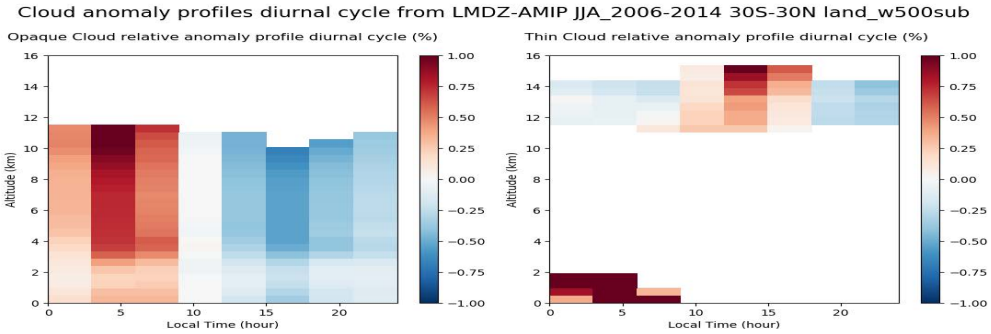

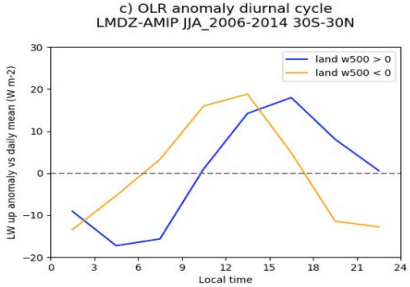

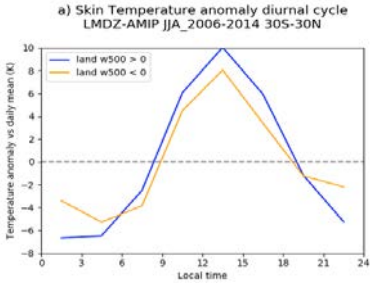

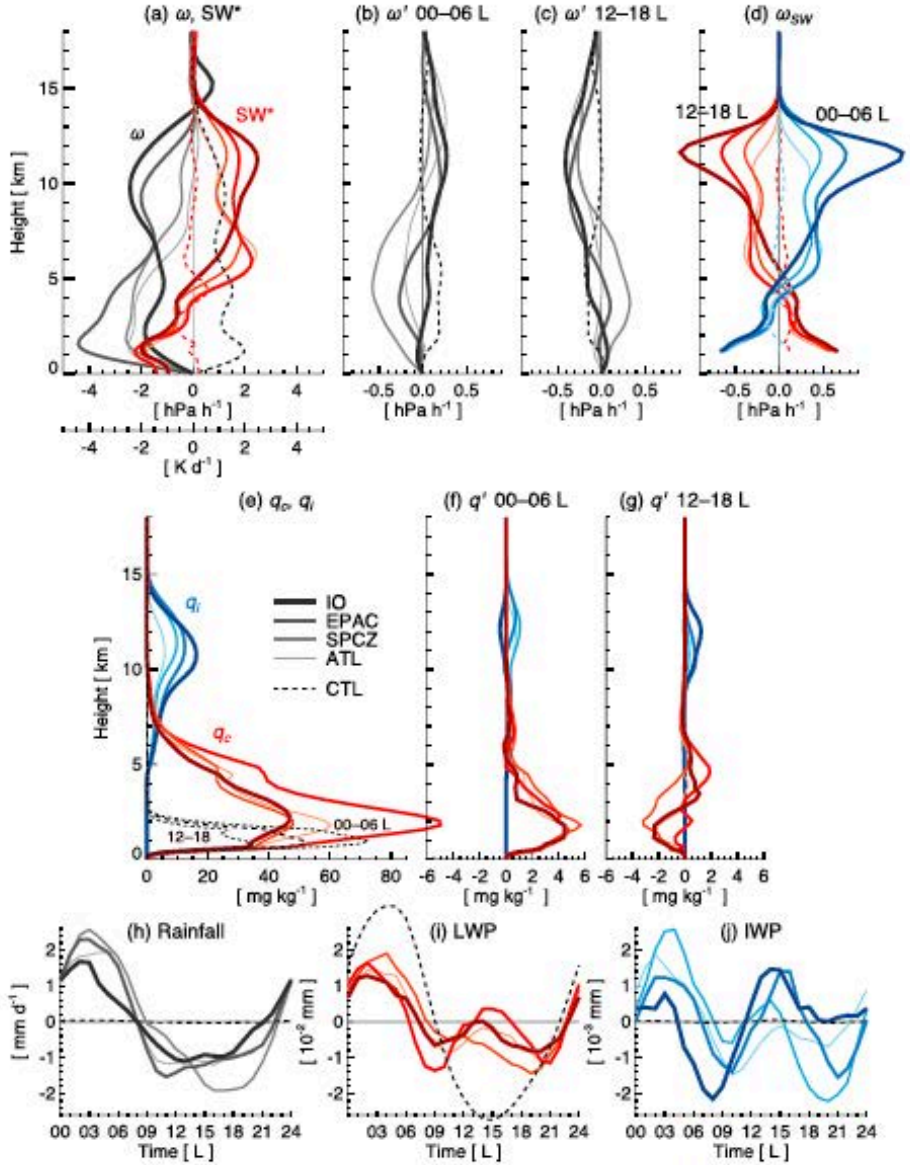

Figure 3. Composites for the selected regions marked by rectangles in Figure 2b, with line thickness and color pigment proportional to magnitude of IWP (or SW*; Figure 1). (a) Mean vertical pressure velocity ω (gray-black; hPa/hr) and SW* averaged from 11–13 L (reds; K/day), and ω' (deviation from daily mean) averaged over (b) 00–06 and (c) 12–18 L. (d) As in (b) and (c) except for the diagnostic motion due to SW ω_{SW}. (e–g) As in (a)–(c) except with cloud liquid water (q_c; red) and cloud ice (q_i; blue; mg/kg). Profiles of q_c and q_i (=0) for CTL are only included in panel (d), with the daily mean (thick dashed) and means for 00–06 and 12–18 L (thin dashed) as labeled. Lastly, time series of (h) rainfall (mm/hr), (i) liquid water path (LWP; 10^{-2} mm), and (j) IWP (10^{-3} mm = g/m^2) with time means subtracted. ATL = Atlantic; CTL = control; EPAC = East Pacific; IO = Indian Ocean; IWP = ice water path; LWP = liquid water path; SPCZ = South Pacific Convergence Zone.

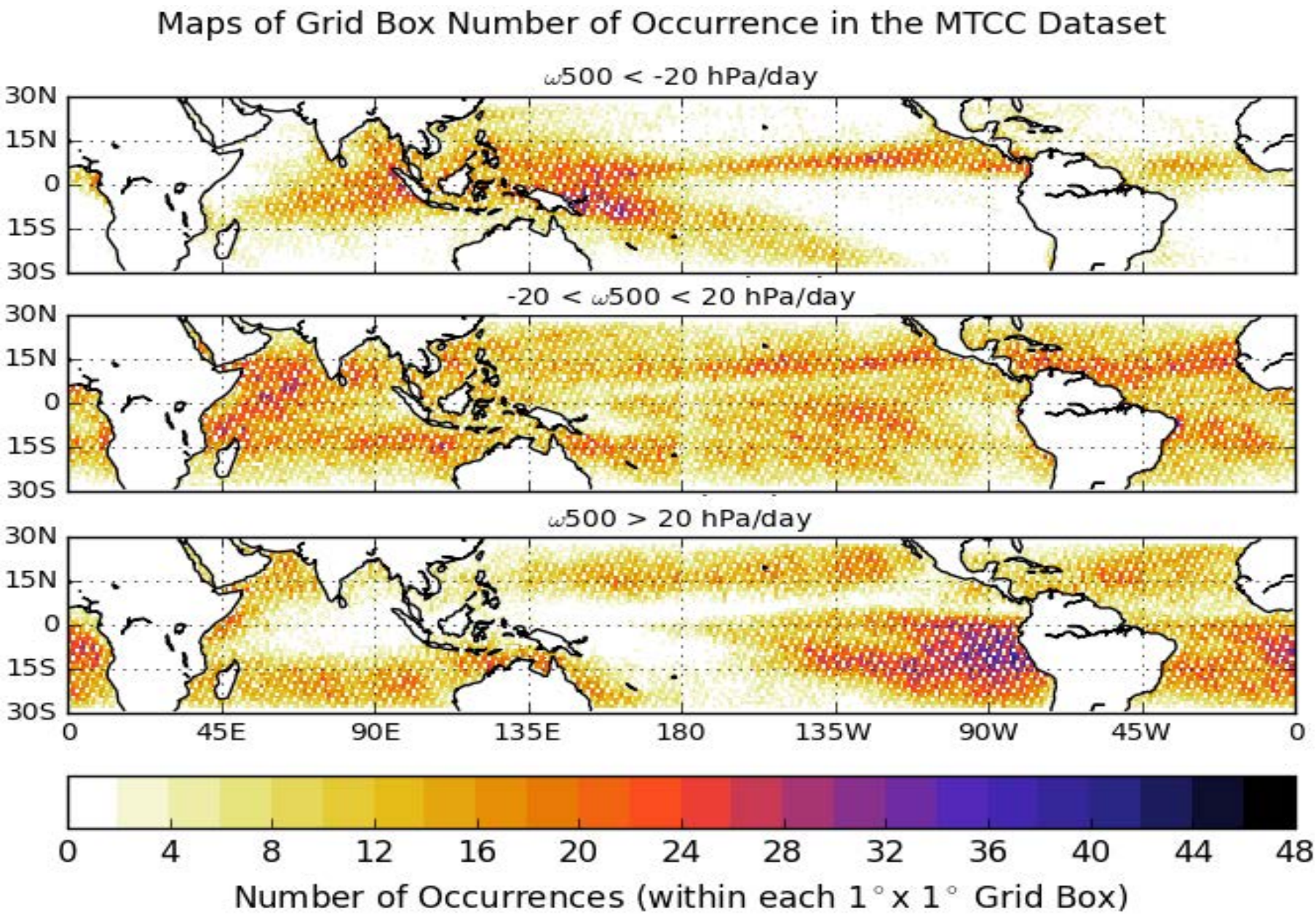
Maps of Grid Box Number of Occurrence in the MTCC Dataset
ω500 < -20 hPa/day
-20 < ω500 < 20 hPa/day
ω500 > 20 hPa/day
30N
15N
0
15S
30S
0
45E
90E
135E
180
135W
90W
45W
0
0
4
8
12
16
20
24
28
32
36
40
44
48
Number of Occurrences (within each 1° x 1° Grid Box)